Optica Applicata, Vol. XXXVII, No. 1, 2007

Calibration free laser-induced breakdown spectroscopy (LIBS) identification of seawater salinity

WALID TAWFIK Y. MOHAMED[1, 2]

[1]National Institute of Laser Enhanced Science (NILES), Dept. of Environmental applications, Cairo University, Cairo, Egypt; e-mail: Walid_Tawfik@hotmail.com

[2]Faculty of Education for girls, Department of Physics, Gurayyat, North of Al-gouf, Kingdom of Saudi Arabia

Laser-induced breakdown spectroscopy (LIBS) has been used as a remote sensing system to analyze seawater samples and to identify their salinities without ordinary calibration curves. The plasma is generated by focusing a pulsed Nd:YAG laser on the seawater surface in air at atmospheric pressure. Such plasma emission spectrum was collected using wide band fused-silica optical fiber of one-meter length connected to a portable Echelle spectrometer (Mechelle 7500 – Multichannel Instruments, Stockholm, Sweden) with intensified CCD camera. Spectroscopic analysis of plasma evolution of laser produced plasmas has been characterized in terms of their spectra, electron density and electron temperature assuming the local thermodynamic equilibrium (LTE) and optically thin plasma conditions. Three elements Na, Ca and Mg were determined in the obtained spectra to identify the salinity of seawater samples. The electron temperature T_e and density N_e were determined using the emission intensity and Stark broadening. The obtained values of T_e and N_e for natural seawater sample (salinity 3.753%) are 11580 K ± 0.35% and 3.33×10^{18} cm^{-3} ± 14.3%. These values exhibit a significant change only if the matrix changes (*i.e.*, the salinity changes). On the other hand, no significant difference was obtained if T_e and N_e were determined using any of the three elements (Na, Ca and Mg) in the same matrix. It is concluded that T_e and N_e represent a fingerprint plasma characterization for a given seawater sample and its salinity could be identified using only one element without need to analyze the rest of elements in the seawater matrix. The obtained results indicate that it is possible to improve the exploitation of LIBS in the remote on-line environmental monitoring, by following up only a single element as a marker to identify the seawater matrix composition and salinity without need to analyze that matrix which saves a lot of time and efforts.

Keywords: laser-induced breakdown spectroscopy (LIBS), matrix effect, remote sensing, plasma parameters, seawater.

1. Introduction

Although a vast majority of seawater is found in oceans with salinity around 3.5%, seawater is not uniformly saline throughout the world. Most of the saline seawater is

due to sodium chloride in addition to calcium and magnesium and some other trace elements like sulfur, potassium, bromine, iodine and carbon. Salinity measurement is very important for many environmental fields, such as marine environment monitoring and quality monitoring of water resources. The measurement of salinity is a complex subject that has a long history. Very briefly, it can be concluded that, in the past, the salinity in seawater was determined by hydrometric methods. In recent years, several methods and technologies have been proposed for salinity measurement [1–5]. For example, an ultrasonic technique [1] based on measurement of the travel-time of light was presented to measure the salinity in solar pond in 1995. A chemical method [2] based on a polyaniline matrix coated wire electrodes was developed for salinity measurement within a range of 0.010% to 75%. The salinity in water was obtained by measuring the potential difference between the coated wire electrode and an Ag/AgCl saturated KCl reference electrode. MINATO *et al.* [3] proposed a fiber-optic system for remote salinity measurement of seawater, which indicated a salinity measurement resolution of 0.02%. ZHAO *et al.* [4, 5] proposed a novel method, which can simultaneously measure the salinity and temperature in water based on optical refraction method. They used a He-Ne laser at 632.8 nm and a position-sensitive detector (PSD) to monitor the beam deviation caused by refraction due to the salinity of measured water at the receiving end face of a measurement cell. The obtained experimental results indicate the feasibility of the developed system with a measurement resolution of 0.012%. In 2006, the author [6] proposed a novel technique, which could simultaneously measure the concentration of Ca, Na, and Mg in seawater. The used technique was laser-induced breakdown spectroscopy (LIBS) that offers unique capabilities for on-line composition determination without sample preparation. In that method, the elemental calibration curves were constructed using the elemental concentration versus its spectral intensity. Moreover, in LIBS, a small volume of the target is intensely heated by the focused beam of a pulsed laser, and thus brought to a transient plasma state where the sample's components are essentially reduced to individual atoms. In this high-temperature plasma, atoms are ionized, or brought to excited states. Such states decay by emission of radiation, which is observed in the ultraviolet (UV), visible and near-infrared (NIR) regions of the spectrum. An atomic spectrum is examined by means of a spectrograph, thereby allowing elemental components of the target to be identified and, quantified using a calibration curve. LIBS measurements are generally carried out in ambient air at atmospheric pressure. For this reason, and also due to its rapidity, non-contact optical nature, and absence of sample preparation, since the only requirement is the optical access to the samples, LIBS is a useful technique for the on-line process analysis. The basic features of this spectroscopic technique and its applications for the on-line measurements have been reviewed in several papers [6–16].

In this paper, LIBS technique will be used as a remote sensor system to measure the salinity of seawater by determining three main elements in saline seawater Na, Ca and Mg without ordinary calibration curves. In the presented sensor system, the plasma

characterization parameters are used to identify the seawater salinity. In doing so, spectroscopic analysis of plasma evolution of laser produced plasmas has been characterized in terms of their spectra, electron density and electron temperature assuming the local thermodynamic equilibrium (LTE) and optically thin plasma conditions.

2. Methodology

A typical LIBS experimental setup, described in details elsewhere [6], is used throughout the present investigations. The plasma formation was attained with the aid of a Q-switched Nd:YAG laser (Continuum NY81.30, USA) delivering laser pulses of 300 mJ/pulse, with 7 ns pulse duration at its fundamental wavelength 1064 nm with adjustable repetition rate up to 30 Hz. The laser pulse energy was adjusted by a suitable combination of neutral filters at constant operating high voltage (1.3 kV) and Q-switch delay (1.5 μs) to ensure spatial and temporal beam profile stability. An energy meter (Nova 978, Ophir Optronics Ltd., USA) was employed to monitor the shot-to-shot pulse energy. Only 180 mJ of the laser pulse energy was focused onto the seawater surface via a quartz plano-convex lens of 100 mm focal length. The emitted light from the plasma plume is collected via a one-meter length wide band fused-silica optical fiber connected to a 0.17 m focal length Echelle spectrometer (Mechelle 7500, Multichannel Instruments, Sweden). The Mechelle 7500 provides a constant spectral resolution of 7500 corresponding to 4 pixels FWHM, over a wavelength range 200–1000 nm displayable in a single spectrum. A gateable, intensified CCD camera, (DiCAM-Pro, PCO Computer Optics, Germany) coupled to the spectrometer was used for detection of the dispersed light. The overall linear dispersion of the spectrometer-camera system ranges from 0.006 nm/pixel (at 200 nm) to 0.033 nm/pixel (at 1000 nm). To avoid the electronic interference and jitters, the CCD intensifier high voltage was triggered optically. The ICCD camera control was performed via Mechelle software (Multichannel instruments, Stockholm, Sweden). The emission spectra display, processing and analysis were done using 2D- and 3D- GRAMS/32 version 5.1 spectroscopic data analysis software (Galactic Industries, Salem, NH, USA).

To improve LIBS precision, spectra from several laser shots have to be averaged in order to reduce statistical error due to laser shot-to-shot fluctuation. As found before by the author [6], all the subsequent measurements must carried out by accumulating fifty spectra for each seawater LIBS spectrum. Moreover, it is found that the optimum delay time for the ICCD Camera is 2500 ns and the gate delay is 10 μs with respect to the laser pulse starting time. Fifty laser shots were fired on the sample surface and the average was computed and saved to serve as the spectrum library. For each recorded spectrum, the peak intensity, the Gaussian curve fitting, the full width at half maximum (FWHM), and the center wavelength of each line, as well as the background emission continuum were determined. Data treatment preprocessing of the averaged spectra was

T a b l e 1. Reference sodium, magnesium and calcium values in ppm for the seawater samples.

Element	Sample-1 (salinity 3.753%)	Sample-2 (salinity 1.876%)	Sample-3 (salinity 0.938%)
Na	11580	5790	2895
Mg	5238	2619	1309.5
Ca	772.8	386.4	193.2

performed in the Microsoft Windows XP environment on a Pentium 4 PC using GRAMS/32, Excel (Microsoft office Excel 2003) and Origin software version 7.0220 (Origin Lab corporation, USA). The averages of peak tables (lists of wavelengths and intensities) of the averaged spectra were roll generated in GRAMS/32 and exported for data evaluation.

Using a classical LIBS configuration, however, as used for LIBS on solids with the laser beam perpendicular to the surface leads to splashing in the case of liquids. The splashing results in covering the focusing optics with droplets and, therefore, prevents further use of this technique. This can easily be explained by the fact that the plasma expansion at atmospheric pressure is directed perpendicularly to the surface [17]. A tilted configuration can minimize this phenomenon. Thus, the Nd:YAG laser beam was focused onto the water surface at 45° angle. This was done using a 25 mm diameter dichroic mirror that reflects 99% of high energy 1064 nm wavelength at angle 45°. Moreover, a low laser pulse repetition rate of 0.2 Hz was used to get rid of any shockwaves produced ripples on the water surface and minimize water splashing too.

On the other hand, the non-contact remote measurements are simulated by using the 100 mm focusing lens and the one meter fused-silica optical fiber (for long range measurements a 3 m focusing lens and a 3 m fused-silica optical fiber could be used instead).

The seawater sample was taken from the Mediterranean sea in the north of Egypt. Then the natural seawater sample was diluted many times with doubly distilled water to obtain a range of salinity. Three samples were selected for measurements and namely: sample-1, sample-2 and sample-3 for natural seawater sample and two diluted seawater samples with dilution ratios (1:1) and (1:3), and salinity values of 3.753%, 1.876% and 0.938%, respectively. The salinities and concentrations of Mg, Ca and Na in these samples were performed on a Varian Spectra AA-220 FS atomic absorption spectrometer (Varian, Australia) and the corresponding values are listed in Tab. 1.

3. Results and discussion

3.1. LIBS spectrum

Figure 1 shows typical LIBS spectra for natural seawater. The three spectra in the figure are plasma emission spectra recorded at 2.5 μs delay time and 10 μs gate width. The panoramic Echelle spectra in the spectral range 250–700 nm made it possible to observe the UV-emission of Mg-lines at 279.55, 280.27 and 285.21 nm, the Ca-lines

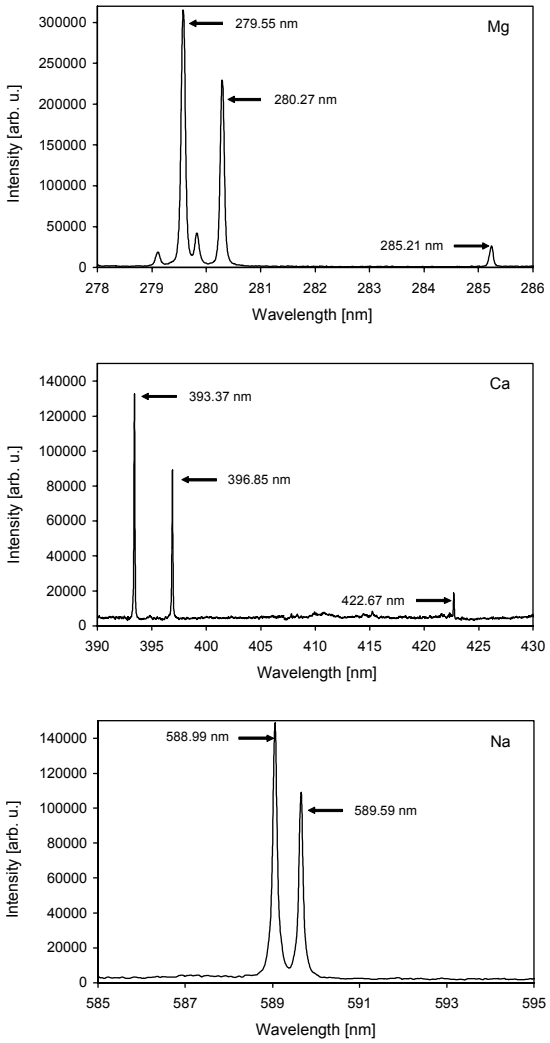

Fig. 1. Typical LIBS spectra for natural seawater sample in the spectral range 278–600 nm for Mg, Ca, and Na, respectively. The laser energy was 180 mJ at wavelength 1064 nm, plasma emissions are accumulated with delay 2.5 μs, and gate width 1 μs.

at 393.37, 396.85 and 422.67 nm, and the well resolved visible Na-lines at 588.99 and 589.59 nm at the same time. The spectra reflect the wide spectral range and the high resolution of the used spectroscopic system.

3.2. Plasma characterization measurements and matrix effect

One of the main problems in the use of LIBS is the necessity of making a calibration curve with samples possessing the same matrix composition as that of the samples to be analyzed. In 1998, BULATOV *et al.* [18] proposed a method in which the composition

of a sample could be determined without the need of calibration curves. They suggested that the matrix effects are due to the higher emission from easily ionized elements existing in the matrix, which contribute to the first stages of plasma formation. However, this method is based on the measurement of the emission from all the species present in the sample, a requirement difficult to satisfy when dealing with *in situ* measurements of natural seawater samples. Understanding of the matrix effect is important to maximize LIBS analytical performance and to determine the technique limitations. The matrix effect can results in the sample being ablated differently from the target sample. The interaction between the laser and the target in LIBS is influenced significantly by the overall composition of the target, so that the intensity of the emission lines observed is a function of both the concentration of the elements of interest and the properties of the matrix that contains them. Plasma composition is dependent not only on the composition of the sample, but also on laser parameters, sample surface conditions as well as on thermal and optical properties of the sample. Previously published works studied the matrix effect under different experimental conditions to specify causes and find out the methods of correction [11, 18–24].

The different approaches have been undertaken to discriminate the problems resulting from the fractionation of the ablation and matrix effects. The most convenient approach is to determine elemental abundance comparing the analyzed line intensities with signals obtained from the proper reference standards having the similar matrix composition. But, it is not always possible to obtain such calibration curves because there are no available standard samples, or it is impossible to have an internal standard of known concentration. In addition, plasma formation dynamics, sample ablation and associated processes are highly non-linear and not fully understood and may also play an important role as reasons of the matrix effect. Thus, in spite of many advantages of LIBS the realization of a quantitative analytical method, which is able to measure main constituents in samples from different matrices, still remains a difficult task because of the complex laser-sample and laser-plasma interaction mechanisms. As a rule, laser ablation plasma is characterized by complex spatial and temporal structures, and one meets a wide range of varying of parameters during the plasma existence time [24].

Below, we will study the dependence of the plasma parameters (electron density, electron temperature) on the matrix composition of the seawater samples. Because if a relation could be found, one can use it to distinguish between different seawater matrices.

3.2.1. Electron temperature and matrix effect

In LIBS experiments, after the initial plasma decay and during the entire observation interval, the local thermodynamic equilibrium (LTE) conditions are assumed to hold.

For optically thin plasma, the re-absorption effects of plasma emission are negligible. So, the emitted spectral line intensity I is a measure of the population of the corresponding energy level of this element in the plasma. For the LTE plasma,

the population of an excited level can be related to the total density $N(T)$ of neutral atom or ion of this element by Boltzmann equation as:

$$I = \frac{hc}{4\pi\lambda} N(T) \frac{A_{ki} g_k}{U(T)} \exp\left(-\frac{E_k}{KT}\right) \tag{1}$$

where λ is the wavelength, A_{ki} is the transition probability, g_k is the statistical weight for the upper level, E_k is the excited level energy, T is the temperature (in LTE all temperatures are assumed to be equal, *i.e.,* $T_e \approx T_{\text{ion}} \approx T_{\text{plasma}}$), K is the Boltzmann constants, $U(T)$ is the partition function [25].

The emitted spectral line intensity from a given state of excitation can be used to evaluate the plasma temperature. The lines must be well resolved in order to accurately

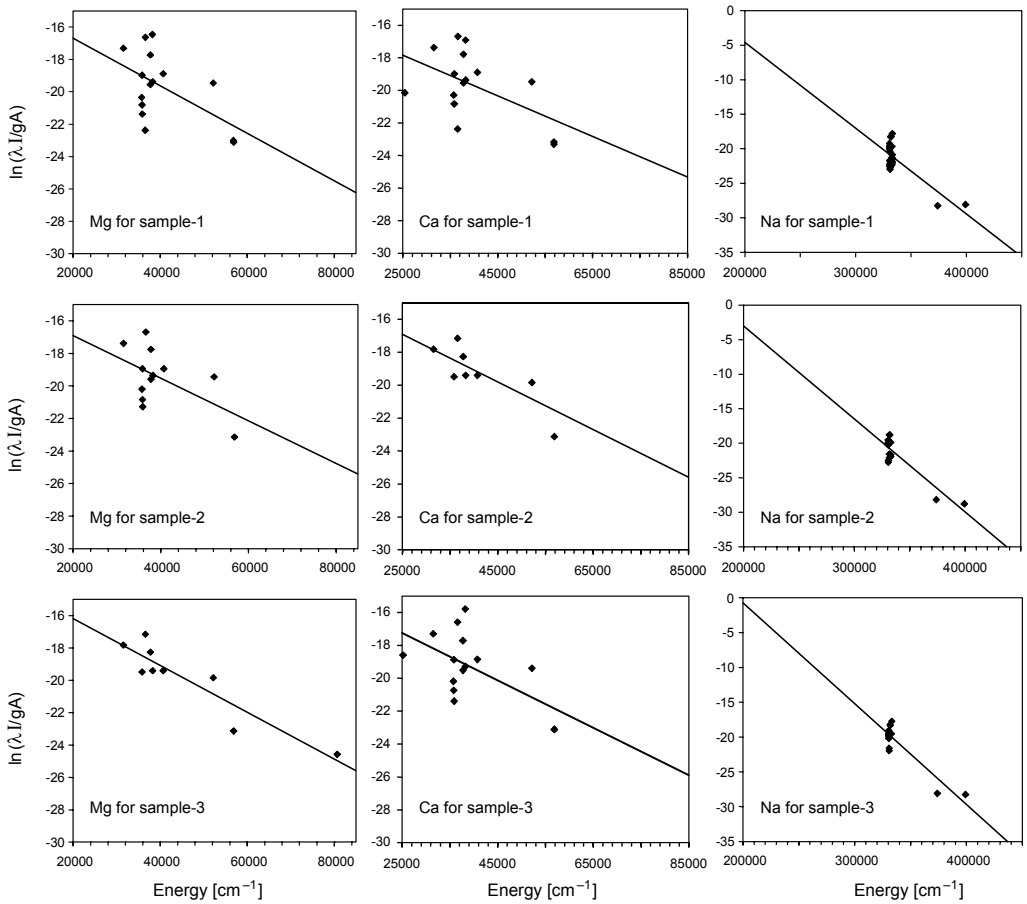

Fig. 2 Nine Boltzmann plots were determined form the emission line intensities of Mg, Ca and Na observed in the laser-induced plasma of seawater samples; sample-1, sample-2, and sample-3 respectively.

T a b l e 2. A list of the spectroscopic data of the spectral lines used for the determination of plasma temperature and density of seawater samples..

Element	Wavelength [nm]	A_{ki} [s^{-1}]	E_k [cm^{-1}]	g_k
Pb	240.19	2.79×10^{7}	49439.62	3
Pb	244.62	2.45×10^{7}	48686.93	3
Pb	247.63	3.78×10^{7}	48188.63	5
Pb	257.73	6.68×10^{7}	49439.62	3
Pb	261.37	1.87×10^{7}	46068.44	3
Pb	261.42	2.35×10^{8}	46060.84	5
Pb	262.83	5.59×10^{7}	48686.93	3
Pb	265.71	9.91×10^{5}	45443.17	5
Pb	266.32	1.01×10^{8}	48188.63	5
Pb	280.19	1.08×10^{8}	46328.67	7
Pb	282.32	3.04×10^{7}	46060.84	5
Pb	283.31	5.92×10^{7}	35287.22	3
Pb	287.33	4.15×10^{7}	45443.17	5
Pb	357.27	4.08×10^{8}	49439.62	3
Pb	363.96	3.20×10^{7}	35287.22	3
Pb	367.15	1.11×10^{8}	48686.93	3
Pb	368.35	1.70×10^{8}	34959.91	1
Pb	373.99	8.30×10^{7}	48188.63	5
Pb	401.96	3.55×10^{7}	46328.67	7
Pb	405.78	9.12×10^{7}	35287.22	3
Pb	406.21	1.07×10^{8}	46068.44	3
Si	221.89	3.55×10^{7}	46328.67	7
Si	243.87	9.12×10^{7}	35287.22	3
Si	250.69	1.07×10^{8}	46068.44	3
Si	251.43	1.50×10^{6}	45276.18	9
Si	251.61	7.40×10^{5}	40991.88	7
Si	252.41	4.66×10^{7}	39955.05	7
Si	252.85	6.10×10^{7}	39760.28	9
Si	288.15	1.21×10^{8}	39955.05	9
Si	300.67	1.81×10^{8}	39683.16	7
Si	302.00	7.70×10^{7}	39760.28	11
Si	390.55	1.89×10^{8}	40991.88	3
Mg	277.66	1.32×10^{8}	57873.94	5
Mg	277.82	1.82×10^{8}	57833.4	3
Mg	277.98	4.09×10^{8}	57873.94	5
Mg	278.14	5.43×10^{8}	57812.77	1
Mg	278.29	2.14×10^{8}	57833.4	3
Mg	279.07	4.01×10^{8}	71491.06	4
Mg	279.55	2.60×10^{8}	35760.88	4

T a b l e 2. Continued.

Element	Wavelength [nm]	A_{ki} [s^{-1}]	E_k [cm^{-1}]	g_k
Mg	279.79	4.79×10^8	71490.19	6
Mg	280.27	2.57×10^8	35669.31	2
Mg	281.11	1.96×10^8	83520.47	5
Mg	281.17	2.11×10^8	83511.25	3
Mg	285.21	4.91×10^8	35051.26	3
Mg	291.54	4.09×10^8	80693.01	5
Mg	292.86	1.15×10^8	69804.95	2
Mg	293.65	2.30×10^8	69804.95	2
Mn	258.97	2.6×10^8	38543.08	7
Mn	401.81	2.54×10^7	41932.64	8
Mn	403.08	1.70×10^7	24802.25	8
Mn	403.31	1.65×10^7	24788.05	6
Mn	403.45	1.58×10^7	24779.32	4
Mn	404.14	7.87×10^7	41789.48	10
Mn	404.88	7.50×10^7	42143.57	4
Mn	405.55	4.31×10^7	41932.64	8
Mn	405.89	7.25×10^7	42198.56	2
Mn	406.17	1.90×10^7	49415.35	6
Mn	406.35	1.69×10^7	42053.73	6
Mn	407.92	3.80×10^7	42143.57	4
Mn	408.29	2.95×10^7	42053.73	6
Mn	408.36	2.80×10^7	41932.64	8
Mn	423.51	9.17×10^7	46901.13	6
Mn	441.49	2.93×10^7	45940.93	6
Mn	445.16	7.98×10^7	45754.27	8

evaluate their wavelengths λ, intensities I, and their transition probabilities A_{ki} must be well known [26].

Reformulating Eq. (1) gives:

$$\ln\frac{I\lambda}{A_{ki}g_k} = -\frac{1}{KT}E_k + \ln\frac{CF}{U(T)} \tag{2}$$

where F is an experimental factor and C is the species concentration.

By plotting the left hand side of Eq. (2) *vs*. the excited level energy E_k, the plasma temperature can be obtained from the slope of the obtained straight line.

The plasma temperatures were determined form the emission line intensities of Ca, Na, and Mg observed in the laser-induced plasma of seawater samples. Here, we aimed at studying the matrix effect on the plasma temperature. In doing so, the plasma

T a b l e 3. The electron temperature T_e determined from the observed magnesium, calcium, and sodium spectral lines in the three seawater samples.

Element	Sample-1	Sample -2	Sample -3
Mg	11603 K	10697 K	9900 K
Ca	11547 K	10681 K	9983 K
Na	11575 K	10665 K	9942 K
Average temerature	11580 K ± 0.35%	10680 K ± 0.37%	9940 K ± 0.43%

temperatures were determined for these elements in the three seawater matrices sample 1, 2 and 3, respectively. Figure 2 shows nine Boltzmann plots of Eq. (2), for these three elements in the three seawater samples where the data were fitted with the least-square approximation. The spectral lines wavelengths, energies of the upper levels, statistical weights, and transition probabilities used for each element were obtained from GRIEM [26], NIST [27] and Kurucz Atomic Line Database [28], and listed in Tab. 2. The slope of the plotted curves yields electron temperature values for the elements Ca, Na, and Mg in each of the three seawater samples as listed in Tab. 3. The average values of the plasma temperature are 11580 K ± 0.35%, 10680 K ± 0.37%, and 9940 K ± 0.43% for seawater samples 1, 2, and 3, respectively. The obtained plasma temperature values agree with the values obtained by the author before [6]. The slightly difference in the plasma temperature values of the three elements is very small (< 0.5%) in the same matrix. Since we assumed the LTE conditions, the obtained small difference in the plasma temperature could be attributed to some experimental errors. On the other hand, there is significant change in the plasma temperature (10–25%) if the matrix changes. This could be understood as follows: for optically thin plasma, any change in the sample matrix produces a change in the physical and chemical properties of the target. This, in turn, affects the energy distribution during the plasma generation and results in a change in the plasma parameters (T_e, N_e) as proved previously by the author group MARWA *et al.* [11] for the case of solid state matrices under conditions similar to the present conditions.

3.2.2. Electron density measurements and matrix effect

The usual method for determination of electron density is the measuring of the broadening of a suitable emission line of the laser-plasma spectrum. There are several possible mechanisms of line broadening in plasma: self-absorption, pressure broadening, Doppler broadening, Stark broadening, *etc*. Lida reported that the line broadening and the spectral shift of the emission line are due mainly to self-absorption phenomenon [29]. In the present study line splitting and the spectral shift, which provide a good evidence of self-absorption, were monitored carefully. No evidence of line splitting or spectral shift was observed.

NEMET and KOZMA [30] reported the broadening of transition lines as pressure, Stark, and Doppler broadening. But pressure and Doppler broadening should not be so much distinguished among transition lines as it is the case for plasma of solids. KYUSEOK SONG *et al.* [31] stated that Stark broadening may be one of the reasons since the broadening effect increases with the increase of the energy level. Stark broadening results from Coulomb interactions between the radiator and the charged particles present in the plasma. Both ions and electrons induce Stark broadening, but electrons are responsible for the major part because of their higher relative velocities. Therefore, in our conditions, the profile of a line is mainly contributed to line widths arises from the Stark effect while the contribution of other mechanisms of broadening (Doppler effect, Van der Waals broadening, and resonance broadening) can be neglected.

The electrons in the plasma can perturb the energy levels of the individual ions which broaden the emission lines originating from these excited levels. Stark broadening of well-isolated lines in the plasma is, thus, useful for estimating the electron number densities provided that the Stark-broadening coefficients have been measured or calculated.

Since the instrumental line-broadening exhibit Gaussian shape, then the Stark line width $\Delta\lambda_{\mathrm{FWHM}}$ can be extracted from the measured line width $\Delta\lambda_{\mathrm{observed}}$ by subtracting the instrumental line broadening $\Delta\lambda_{\mathrm{instrument}}$:

$$\Delta\lambda_{\mathrm{FWHM}} = \Delta\lambda_{\mathrm{observed}} - \Delta\lambda_{\mathrm{instrument}} \tag{3}$$

In our case $\Delta\lambda_{\mathrm{instrument}}$ was 0.05 nm (determined by measuring the FWHM of the Hg lines emitted by a standard low pressure Hg lamp).

The width of Stark broadening spectral line depends on the electron density N_e. Both the linear and the quadratic Stark effect are encountered in spectroscopy. Only the hydrogen atom and H-like ion exhibit the linear Stark effect. For the linear Stark effect the electron density should be deduced from H line width from the formula [26]

$$N_e = C(N_e, T)\Delta\lambda_{\mathrm{FWHM}}^{3/2} \tag{4}$$

The values of the parameter $C(N_e, T)$ are tabulated in [21], which determine the relative contribution of the electron collision to the electrostatic fields, and depend weakly on N_e and T.

For a non-H-like line, the electron density (in cm^{-3}) could be determined from the FWHM of the line from the formula [26]:

$$N_e \approx \frac{\Delta\lambda_{\mathrm{FWHM}}}{2w} \times 10^{16} \tag{5}$$

where w is the electron impact parameter (Stark broadening value).

T a b l e 4. The plasma electron density N_e determined from the observed calcium, magnesium, and sodium spectral lines in the three seawater samples.

Element	Wavelength [nm]	Stark broadening parameter [nm]	Sample-1 [cm^{-3}]	Sample-2 [cm^{-3}]	Sample-3 [cm^{-3}]
Ca	422.67	7.18×10^{-4}	3.75×10^{18}	6.05×10^{17}	2.42×10^{17}
Mg	285.21	4.13×10^{-4}	2.85×10^{18}	5.92×10^{17}	2.78×10^{17}
Na	297.50	8.85×10^{-5}	3.38×10^{18}	6.21×10^{17}	2.82×10^{17}
Average N_e			$3.33\times10^{18} \pm 14.3\%$	$6.03\times10^{17} \pm 2.6\%$	$2.67\times10^{17} \pm 9.4\%$

The same three elements were taken into consideration for electron density measurements at wavelengths 422.67, 285.21 and 297.50 nm for Ca, Mg, and Na, respectively. The three candidates lines data points were fitted with Gaussian fitting function using the Origin software (version 7.0220, Origin Lab corporation, USA) to determine $\lambda_{1/2}$ (the wavelength of full width at half-maximum). The Stark broadening W values are taken from GRIEM [26] at electron temperature of 10000 K and listed in Tab. 4. Substituting the values of $\lambda_{1/2}$ and the corresponding value of Stark broadening W in Eq. (5), the electron densities for Ca, Mg, and Na were determined. These steps were repeated for each of the seawater samples. The obtained electron density values are listed in Tab. 4 and the average values of the plasma density are 3.33×10^{18} cm^{-3} ± 14.3%, 6.03×10^{17} cm^{-3} ± 2.6% and 2.67×10^{17} cm^{-3} ± 9.4% for seawater samples 1, 2, and 3, respectively. Since we assumed the LTE conditions, the slight difference in the plasma density values of the three elements (Na, Ca, and Mg) is small (2.6–14.3%) in the same matrix which could be attributed to the experimental errors. On the other hand, there is a significant change in the plasma density up to order of magnitude if the matrix changes. This could be understood, as stated for the case of plasma temperature, that any change in the sample matrix produces a change in the physical and chemical properties of the target and, in turn, affects the energy distribution during the plasma generation and results in a change in the plasma parameters (T_e, N_e) [6].

Finally, by knowing the electron density and the plasma temperature we can determine whether LTE assumption is valid applying the criterion given by MCWHIRTER [32]. The lower limit for electron density for which the plasma will be in LTE is:

$$N_e \geq 16 \times 10^{12} \Delta E^{1/3} T^{1/2} \tag{6}$$

where ΔE is the largest energy transition for which the condition holds and T is the plasma temperature [15]. In the present case ΔE = 4.9 eV for Mg at 279.55 nm (see Tab. 2) and its electron density lower limit value given by Eq. (6) is 1.88×10^{16} cm^{-3} (see ref. [11]). The experimentally calculated densities are greater than this value, which is consistent with the assumption that the LTE is prevailing in the plasma.

4. Conclusions

In the present work, we used an accurate LIBS setup to identify different seawater samples (with different salinities) using an optical fiber probe. In doing so, we study the matrix effect on the plasma characterization of seawater samples. The obtained results showed that both electron temperature and density are related to the matrix composition and change if the matrix changes. Moreover, T_e and N_e could be measured using any of the three elements (Na, Ca, and Mg) in the seawater matrix. This means that T_e and N_e represent a fingerprint plasma characterization for a given seawater sample and its salinity could be identified using only one element without need of analysis of the rest of elements in the seawater matrix. This could be done by building a database containing the determined values of T_e and N_e for a wide range of seawater salinities. Then the salinity of the unknown seawater sample could be identified just by comparing its measured T_e and N_e values with the previously stored values in our database.

The obtained results indicate that it is possible to improve the exploitation of LIBS in the remote on-line environmental monitoring, by following up only a single element as a marker to identify the seawater matrix composition and salinity without need to analyze that matrix which saves a lot of time and efforts.

Acknowledgment – The author acknowledges Prof. M. Abdel Harith specially for offering the seawater samples.

References

[1] MIN Z.J., LI J.P., JIANG S.H., *Measurement of salt salinity in solar pond by supersonic method*, Acta Eneglae Solaris Sinica **16**(2), 1995, pp. 224–8.

[2] DINIZ F.B., DE FREITAS K.C.S., DE AZEVEDO W.M., *Salinity measurements with polyaniline matrix coated wire electrodes*, Electrochemistry Communications **1**(7), 1999, pp. 271–3.

[3] MINATO H., KAKUI Y., NISHIMOTO A., NANJO M., *Remote refractive index difference meter for salinity sensor*, IEEE Transactions on Instrumentation and Measurement **38**(2), 1989, pp. 608–12.

[4] ZHAO Y., LIAO Y.B., *Novel optical fiber sensor for simultaneous measurement of temperature and salinity*, Sensors and Actuators B: Chemical **86**(1), 2002, pp. 63–7.

[5] ZHAO Y., ZHANG BO, LIAO YANBIAO, *Experimental research and analysis of salinity measurement based on optical techniques*, Sensors and Actuators B: Chemical **92**(3), 2003, pp. 331–6.

[6] TAWFIK Y. MOHAMED W., *Quantitative elemental analysis of seawater by laser induced breakdown spectroscopy*, International Journal of Pure and Applied Physics **2**(1), 2006, pp. 11–21.

[7] RADZIEMSKI L.J., CREMERS D.A., *Laser Induced Plasmas and Applications*, Marcel Dekker, New York 1989.

[8] SOLIMAN M., TAWFIK W., HARITH M.A., *Quantitative elemental analysis of agricultural drainage water using laser induced breakdown spectroscopy*, [In] *First Cairo Conference on Plasma Physics and Applications*, Cairo, Egypt, Forschungszentrum Juelich GmbH, Bilateral Seminars of the International Bureau, Vol. 34, 2003, pp. 240–3.

[9] TAWFIK Y. MOHAMED W., ASKAR A., *Study of the matrix effect on the plasma characterization of heavy elements in soil sediments using LIBS with a portable Echelle spectrometer*, Progress in Physics **1**, 2007, pp. 46–52.

[10] MOHAMAD SABSABI, VINCENT DETALLE, MOHAMED A. HARITH, WALID TAWFIK, HISHAM IMAM, *Comparative study of two new commercial Echelle spectrometers equipped with intensified CCD for analysis of laser-induced breakdown spectroscopy*, Applied Optics **42**(30), 2003, pp. 6094–8.
[11] ISMAIL M.A., IMAM H., ELHASSAN A., TAWFIK Y. MOHAMED W., HARITH M.A., *LIBS limit of detection and plasma parameters of some elements in two different metallic matrices*, Journal of Analytical Atomic Spectrometry **19**(4), 2004, pp. 489–94.
[12] CHARFI B., HARITH M.A., *Panoramic laser-induced breakdown spectrometry of water*, Spectrochimica Acta Part B: Atomic Spectroscopy **57**(7), 2002, pp. 1141–53.
[13] ARCA G., CIUCCI A., PALLESCHI V., RASTELLI S., TOGNONI E., *Trace element analysis in water by laser-induced breakdown spectroscopy technique*, Applied Spectroscopy **51**(8), 1997, pp. 1102–5.
[14] FICHET P., MAUCHIEN P., WAGNER J.-F., MOULIN C., *Quantitative elemental determination in water and oil by laser induced breakdown spectrodcopy*, Analytica Chimica Acta **429**(2), 2001, pp. 269–78.
[15] SAMEK O., BEDDOWS D.C., KAISER J., KUKHLEVSKY S.V., LISKA M., TELLE H.H., YOUNG J., *Application of laser-induced breakdown spectroscopy to in situ analysis of liquid samples*, Optical Engineering **39**(8), 2000, pp. 2248–62.
[16] WISBRUN R., SCHECHTER I., NIESSNER R., SCHROEDER H., *Laser-Induced Breakdown Spectroscopy for Detection of Heavy Metals in Environmental Samples*, Vol. 1716**,** SPIE, Bellingham, Washington, 1992, pp. 2–14.
[17] SALLE B., CHARLEARD C., DETALLE V., LACOUR J.L., MAUCHIEN P., NOUVELLON C., SEMEROK A., *Laser ablation efficiency of metal samples with UV laser nanosecond pulses*, Applied Surface Science **138**–**139**, 1999, pp. 302–5.
[18] BULATOV V., KRASNIKER R., SCHECHTER I., *Study of matrix effects in laser plasma spectroscopy by combined multifiber spatial and temporal resolutions*, Analytical Chemistry **70**(24), 1998, pp. 5302–11.
[19] XU L., BULATOV V., GRIDIN V.V., SCHECHTER I., *Absolute analysis of particulate materials by laser -induced breakdown spectroscopy*, Analytical Chemistry **69**(11), 1997, pp. 2103–8.
[20] GOODE S.R., MORGAN S.L., HOSKINS R., OXSHER A., *Identifying alloys by laser-induced breakdown spectroscopy with a time-resolved high resolution echelle spectrometer*, Journal of Analytical Atomic Spectrometry **15**(9), 2000, pp. 1133–8.
[21] EPPLER A.S., CREMERS D.A., HICKMOTT D.D., FERRIS M.J., KOSKELO A.C., *Matrix effects in the detection of Pb and Ba in soils using laser-induced breakdown spectroscopy*, Applied Spectroscopy **50**(9), 1996, pp. 1175–81.
[22] CIUCCI A., CORSI M., PALLESCHI V., RASTELLI S., SALVETTI A., TOGNONI E., *New procedure for quantitative elemental analyses by laser induced plasma spectroscopy*, Applied Spectroscopy **53**(8), 1999, pp. 960–4.
[23] BULAJIC D., CORSI M., CRISTOFORETTI G., LEGNAIOLI S., PALLESCHI V., SOLVETTI A., TOGNONI E., *A procedure for correcting self-absorption in calibration-free laser induced breakdown spectroscopy*, Spectrochimica Acta Part B: Atomic Spectroscopy **57**(2), 2002, pp. 339–53.
[24] CORSI M., PALLESCHI V., SALVETTI A., TOGNONI E., *Making LIBS quantitative: a critical review of the current approaches to the problem*, Research Advances in Applied Spectroscopy **1**, 2000, pp. 41–7.
[25] SIMEONSSON J.B., MIZIOLEK A.W., *Time-resolved emission. studies of ArF laser-produced micro-plasmas*, Applied Optics **32**(6), 1993, pp. 939–47.
[26] GRIEM H.R., *Plasma Spectroscopy*, McGraw-Hill, New York 1964.
[27] NIST National Institute of Standards and Technology, USA, electronic database, http:// physics.nist.gov/PhysRefData/ASD/lines_form.html.
[28] Kurucz Atomic Line Database, http://www.cfa.harvard.edu/amdata/ampdata/kurucz23/sekur.html.
[29] IIDA Y., *Effects of atmosphere on laser vaporization and excitation processes of solid samples*, Spectrochimica Acta Part B: Atomic Spectroscopy **45**(12), 1990, pp.1353–67.

[30] NEMET B., KOZMA L., *Time-resolved optical emission spectrometry of Q-switched Nd:YAG laser-induced plasmas from copper targets in air at atmospheric pressure*, Spectrochimica Acta Part B: Atomic Spectroscopy **50**(14), 1995, pp. 1869–88.

[31] KYUSEOK SONG, HYUNGKI CHA, JONGMIN LEE, YONG-ILL LEE, *Investigation of the line-broadening mechanism for laser-induced copper plasma by time-resolved laser-induced breakdown spectroscopy*, Microchemical Journal **63**(1), 1999, pp. 53–60.

[32] MCWHIRTER R.W.P., *In Plasma Diagnostic Techniques*, [Eds.] R.H. Huddlestone, S.L. Leonard, Chap. 5, Academic Press, New York 1965, p. 206.

Received January 11, 2007
in revised form March 5, 2007